



**HAL**  
open science

# **EOCONUSPHAERA hallstattensis sp. nov. and a review of the Rhaetian genus EOCONUSPHAERA**

Isaline Demangel, Richard Howe, Silvia Gardin, Sylvain Richoz

► **To cite this version:**

Isaline Demangel, Richard Howe, Silvia Gardin, Sylvain Richoz. *Eoconusphaera hallstattensis* sp. nov. and a review of the Rhaetian genus *Eoconusphaera*. *Journal of Nannoplankton Research*, 2021, 39 (1), pp.77-87. hal-03986488

**HAL Id: hal-03986488**

**<https://hal.science/hal-03986488>**

Submitted on 13 Feb 2023

**HAL** is a multi-disciplinary open access archive for the deposit and dissemination of scientific research documents, whether they are published or not. The documents may come from teaching and research institutions in France or abroad, or from public or private research centers.

L'archive ouverte pluridisciplinaire **HAL**, est destinée au dépôt et à la diffusion de documents scientifiques de niveau recherche, publiés ou non, émanant des établissements d'enseignement et de recherche français ou étrangers, des laboratoires publics ou privés.

# ***Eoconusphaera hallstattensis* sp. nov. and a review of the Rhaetian genus *Eoconusphaera***

## **Isaline Demangel**

Institute of Earth Sciences, University of Graz, NAWI Graz Geocenter, Heinrichstraße 26, 8010 Graz, Austria & Department of Geology, University of Lund, Sölvegatan 12, 22362 Lund, Sweden; isaline.demangel@geol.lu.se

## **Richard Howe**

Ellington Geological Services, 1414 Lumpkin Road, Houston, TX 77043, USA; richard.howe@ellingtongeo.com

## **Silvia Gardin**

Centre de Recherche en Paléontologie, Sorbonne Université, Paris, France; silvia.gardin@upmc.fr

## **Sylvain Richoz**

Institute of Earth Sciences, University of Graz, NAWI Graz Geocenter, Heinrichstraße 26, 8010 Graz, Austria & Department of Geology, University of Lund, Sölvegatan 12, 22362 Lund, Sweden; sylvain.richoz@geol.lu.se

Manuscript received 24th February, 2020; revised manuscript accepted 26th March, 2021

**Abstract** The genus *Eoconusphaera* is among the few calcareous nannofossil genera that occur in the Upper Triassic. The calcareous nannofossil assemblages of three Rhaetian sections—two from the Austrian Northern Calcareous Alps and one from offshore north-western Australia—were studied using scanning electron and/or transmitted-light microscopy. Significant structural differences were observed in the inner structures of conical Rhaetian forms belonging to *Eoconusphaera*, which prompted a revision of *Eoconusphaera zlam- bachensis* and the description of a new species, *E. hallstattensis* sp. nov.

**Keywords** calcareous nannofossils, Upper Triassic, Rhaetian, nannoliths, coccoliths, *Eoconusphaera zlam- bachensis*, *Eoconusphaera hallstattensis*, taxonomy, Tethys Ocean, Tethyan, Austria, Australia

## **1. The Upper Triassic genus *Eoconusphaera*: State of the art and historical background**

The first records of the family Eoconusphaeraceae go back to the 1980s, with the original description of *Conusphaera zlam- bachensis* by Moshkovitz (1982) from the Lower Rhaetian Zlambach Formation of Austria. *Conusphaera zlam- bachensis* was originally described as an elongated cone, truncated at both ends, with an inner part of inclined laths and an outer mantle of vertical, non-imbricating plates. One year later, Jafar (1983) described a new genus and species, *Eoconusphaera tollmanniae*, from the same area and formation. The description and figures (Jafar, 1983, p. 228, figs 1–3) of *E. tollmanniae* correspond very closely with the illustrations of *C. zlam- bachensis* in Moshkovitz (1982, p. 1, figs 1–10).

The genus *Eoconusphaera* was described by Jafar (1983) as differing from the Upper Jurassic–mid-Cretaceous (Tithonian–Aptian) genus *Conusphaera* in having a dome at the broader end and lacking an axial ‘canal’. Numerous published illustrations of *Conusphaera mexicana* (e.g. Bown & Cooper, 1989, pl. 5.2, fig. 4) show that it can have a domed shape at its wide end, so this criterion cannot be used to separate the two genera. *Conusphaera* also lacks an axial canal, in the sense of an axial cavity running vertically through the centre of the conical nannofossil. A dark optical suture, rather than a central canal, can be seen along the axis when viewed under crossed-nicols in the light-microscope (LM) (e.g. Bown & Cooper, 1989, pl. 4.16, fig. 3). This optical suture is simply the axis from which the calcite laths that comprise the central core radiate, and it is similar in both *Conusphaera* and *Eoconusphaera zlambachensis*. For these reasons, the two genera cannot be separated in the way intended by Jafar (1983), but can instead be separated by the inclination of the inner laths (Moshkovitz, 1982) and their disjunct stratigraphic occurrence.

Posch & Stradner (1987) discussed the detailed structure of *E. zlambachensis* and showed that the outer mantle consists of elongated, smooth, vertically-oriented plates enclosing an inner core made of seven or eight bundles of thin calcite laths that are obliquely stacked within each bundle—an ultrastructure that is unique to *E. zlambachensis*.

Janofske (1987) regarded the genus *Eoconusphaera* as superfluous, recombining *E. tollmanniae* into *Conusphaera*. She regarded the species *zlambachensis* and *tollmanniae* as differing in the orientation of their inner laths—vertical in *tollmanniae* and inclined in *zlambachensis*. This distinction between the two species is not clearly shown in any of her illustrations, however, and has not been followed subsequently. Kristan-Tollmann (1988) regarded *E. tollmanniae* as being a junior synonym of *C. zlambachensis*, making *C. zlambachensis* the type species of *Eoconusphaera* when she recombined it into *Eoconusphaera*.

A new investigation of Upper Triassic sediments from the Steinbergkogel and Zlambach sections in the Northern Calcareous Alps (NCA, Austria) has led to the observation of two different conical forms. To clarify the taxonomy and descriptions of the species belonging to the genus *Eoconusphaera*, we investigated them using both scanning electron and transmitted-light microscopy in order to observe and describe in detail the ultrastructural characteristics of these species. We added and compared LM observations made on another section, from the Northern Carnarvon Basin (NCB) in Australia, to give a more global perspective to our descriptions.

## 2. Materials and methods

During the Rhaetian (208.5–201.4 Ma; Ogg & Chen, 2020), the Austrian sections were located around 25°N (Gallet et al., 1996), on the western margin of the Neo-Tethys Ocean, whilst the Australian sections from the NCB, were located at around 30°S, along the southern margin of the Neo-Tethys Ocean. Of the two Austrian sections analysed, the Steinbergkogel section (47.5639°N, 13.6261°E) is located west of Lake Hallstatt, at around 1245 masl (Figure 1). It represents a topographic high, with red condensed limestone in a deep ramp setting (Richoz & Krystyn, 2015; Demangel et al., 2020;

Kovács et al., 2020). The chronologically younger Kleiner Zlambach section (47.6389°N, 13.6593°E) is located 3 km north of Lake Hallstatt, along the Kleiner Zlambach River, at around 870 masl (Figure 1), and represents a toe-of-slope palaeosetting, with limestone and marl deposition (Richoż & Krystyn, 2015; Galbrun et al., 2020; Kovács et al., 2020).

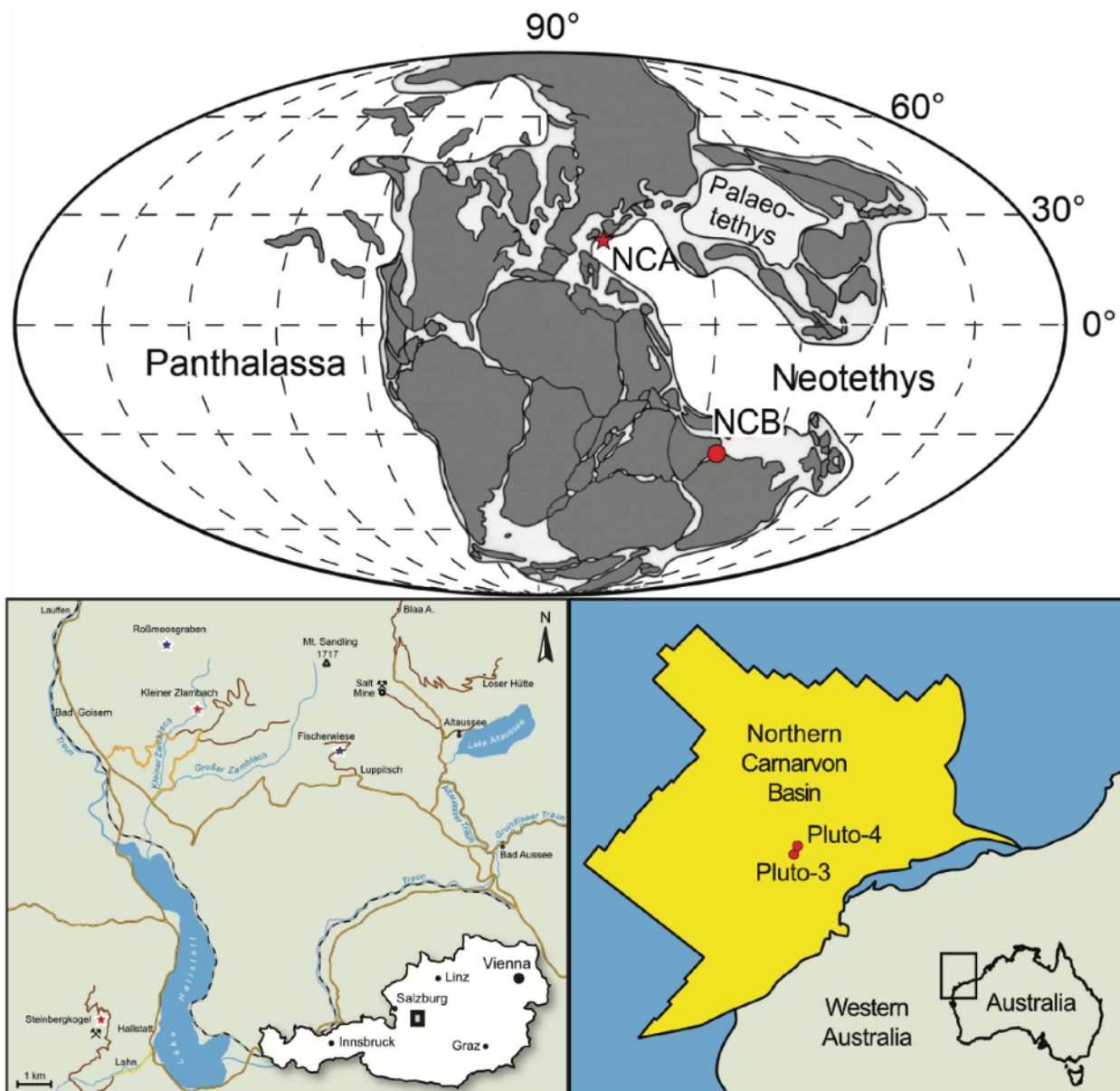


**Figure 1:** **A)** Global map of the Late Triassic showing the NCA (red star) and NCB (red circle) (modified after Scotese, 2004; Golonka, 2007; Nakada et al., 2014). **B)** Simplified map of Austria showing the studied sections (red stars) and two localities cited in the literature (blue stars) (modified after Gardin et al., 2012). **C)** Map of north-western Australia, showing the location of Pluto-3 and 4 in the NCB (red circles) (modified after Marshall & Lang, 2013)

The Australian material is from the Pluto-3 and 4 petroleum exploration wells (Woodside, 2007a, b), drilled in the NCB, offshore Western Australia. Pluto-3 was drilled in 584.6 m water depth at -19.9119°S, 115.1613°E, whilst Pluto-4 was drilled in 970.6 m water depth at 19.8487°S, 115.165°E. The samples studied here came from conventional cores taken from the Brigadier Formation, an offshore marine marl, deposited in a wide and shallow epicontinental sea between Australia and Greater India (Marshall & Lang, 2013). The

Brigadier Formation is Rhaetian in age, based on the *Ashmoripollis reducta* spore/ pollen zone and the *Dapcodinium priscum* and *Rhaetogonyaulax rhaetica* dinoflagellate zones, correlated to the Rhaetian by Helby et al. (1987, 2004).

A total of 55 samples were analysed from Austria—24 from the 28-m-thick Steinbergkogel section and 31 from the 55-m-thick Zlambach section. Two samples were examined from north-western Australia, from cores taken from the petroleum exploration wells, Pluto-3 and 4. Smear-slides of the Austrian samples were prepared following the description of Bordiga et al. (2015). Fresh rock surfaces were powdered, and 0.05 g of the rock powder was mixed with 50 ml of buffered ammonia. With a micro-pipette, 1.5 ml of the solution were placed on a coverslip and homogenised by aspiration and release. The coverslip was dried slowly, below 50°C, to avoid sediment aggregates from forming, then mounted on a slide using Norland Optical Adhesive before curing using a UV lamp. For the Australian samples, smear-slides were prepared following the method of Bown & Young (1998). LM observations were performed on the Austrian samples using an Olympus BX50 microscope at a magnification of 2500x, and on the Australian samples using a Leitz Ortholux microscope at a magnification of 1000x. The scanning electron microscope (SEM) samples were prepared mainly following the method of Preto et al. (2013a, b). The samples were cut into 1-cm<sup>2</sup> blocks and polished with 600- and 1200-diamond discs using deionised water as a lubricant. These blocks were etched for 15 s in 0.1% HCl and cleaned for 7 s in an ultrasonic bath with distilled water. The samples were dried overnight in an oven at 50°C and finally coated with 1 nm of platinum/palladium using a Cressington Sputter Coater 208HR. The observations were performed using a TESCAN MIRA 3 electron microscope at Lund University.

### 3. Systematic palaeontology

The studied sections contain several calcareous nannofossil species characteristic of the Rhaetian. The spherical nannolith *Prinsiosphaera triassica* is abundant, as are the two species of *Eoconusphaera* described here—*E. zlambachensis* and *E. hallstattensis* sp. nov. Three species of coccolithophorids were also observed—*Crucirhabdus minutus*, *C. primulus* and *Archaeozygodiscus koessenensis*. Three calcisphere species were also present—*Thoracosphaera* sp., *Obliquipithonella* sp. and *Orthopithonella* sp.

The species belonging to the genus *Eoconusphaera* are considered by most workers to be nannoliths of unknown affinity. However, the following evidence suggests a likely affinity to the coccolithophorids. Their morphology (conical shape, outer mantle with narrow vertical elements, core comprising complexly arranged elements, and also size; Figure 2) is similar to the coccolith species *Calcivascularis jansae* Wiegand, 1984, which occurs in the Lower Jurassic (Sinemurian–Lower Toarcian). Although *C. jansae* has a similar overall morphology to *Eoconusphaera*, it is not closely related, as its evolution from the protolith coccolith genus *Mitrolithus* is well understood (Young et al., 1986; Bown, 1987). *Eoconusphaera* and the coccolithophorids seem to have a similar palaeoenvironmental preference, evolving first in subtropical zones (Jafar, 1983; Gardin et al., 2012; Demangel et al., 2020), and migrating into the tropical zone only during the latest Rhaetian, while other nannoliths, such as *P. triassica*, were present in both zones since the Norian (Jafar, 1983; Bralower et al., 1991). However, these species cannot be assigned to either

*Crucirhabdus* or *Archaeozygodiscus*. The absence of a proximal cycle in the specimens observed with the LM prevented us from inferring a clear affinity to *Crucirhabdus*, and the presence of an outer cycle of vertical, non-imbricating elements does not correspond to *Archaeozygodiscus*. The optical birefringence was investigated under polarised light with a gypsum plate to determine the crystallographic orientation.

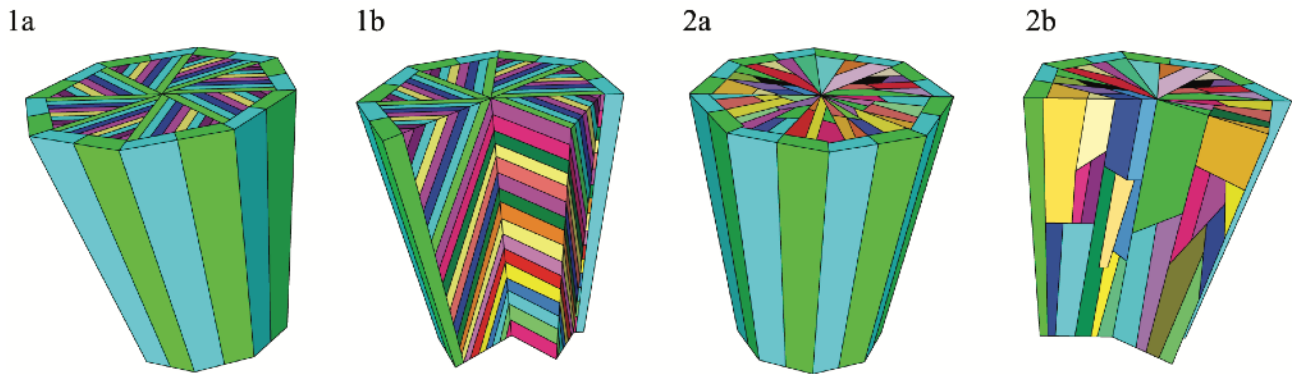


**Figure 2:** Schematic representations of 1) *Eoconusphaera z lambachensis* and 2) *E. hallstattensis*, showing (a) the outer mantle and top view and (b) the inner core, indicating the orientation of the inner laths. Note that the colours aid visualisation of the structure, but have no particular significance

In both species, the outer mantle in the N–S position appears yellow on the left-hand side and blue on the right-hand side (*E. hallstattensis*—Pl. 1, figs 15d, 17b; *E. z lambachensis*—Pl. 2, figs 10b, 11b, 13d, 14b), then goes into extinction at 45° (*E. hallstattensis*—Pl. 1, figs 15b, 17d; *E. z lambachensis*—Pl. 2, figs 10d, 13b, 14d). This information suggests sub-radial orientations with tapering *c*-axes for the outer mantle. The inner core elements show minimum birefringence in the N–S and E–W positions, then yellow at 45°, suggesting sub-vertical *c*-axes. This set of orientations is common among the Upper Triassic coccoliths (Young et al., 1992), providing new evidence for an affinity between them and *Eoconusphaera*.

The formal definition of our new species is presented below, in accordance with the International Code of Nomenclature for algae, fungi, and plants (Shenzhen Code) (Turland et al., 2018).

#### Family **EOCONUSPHAERACEAE** Kristan-Tollmann, 1988

Genus *Eoconusphaera* Jafar, 1983 *Eoconusphaera hallstattensis* sp. nov. **Pl. 1, figs 1–18**

1991 *Eoconusphaera z lambachensis* (Moshkovitz, 1982) Bown & Cooper, 1989 – Bralower et al.: pl. IX, figs 7–11, ?non fig. 6.

2012 *Eoconusphaera z lambachensis* (Moshkovitz, 1982) Kristan-Tollmann, 1988 – Gardin et al.: figs 6 J–I. 2020 *Eoconusphaera hallstattensis* (Moshkovitz, 1982) Kristan-Tollmann, 1988 – Demangel et al.: fig. 5A.

**Derivation of name:** After the Hallstatt Formation, NCA, Austria, where the first specimens of this new species were found. **Diagnosis:** Elliptical (Pl. 1, fig. 3) to subcircular (Pl. 1, fig. 8) conical nannofossil, truncated at both ends, with a flat to domed

distal end (Pl. 1, figs 1, 7, 10–12, 14– 16, 18). The outer mantle of elements is composed of tall, flat laths, vertically oriented without imbrication or overlap (Pl. 1, figs 1, 3, 4, 7, 9, 10). The number of outer elements observed is at least 12–14, although overgrowth can obscure this number. The inner core is composed of tall, thin elements that are oriented vertically to sub-vertically, appearing radial in plan view. No canal is visible, only a central suture that corresponds to the axis of radiation of the inner core laths (Pl. 1, figs 3, 8, 16, 18). The inner elements are of different lengths, and irregularly overlap each other. They end in a flat to domed shape on the wide end of the truncated cone. Under the LM, this species presents a trapezoid shape, with the flat outer mantle clearly visible, and showing first-order grey birefringence (Pl. 1, figs 2, 11–18). The inner part appears to be composed of several undulating bars of different lengths or small blocks, which are parallel to the outer mantle elements. The undulating effect is a result of the bundles of overlapping inner elements. At the wide end of the nannofossil, the core can protrude beyond the outer mantle (Pl. 1, figs 1, 10, 14, 15, 16c, 18a).

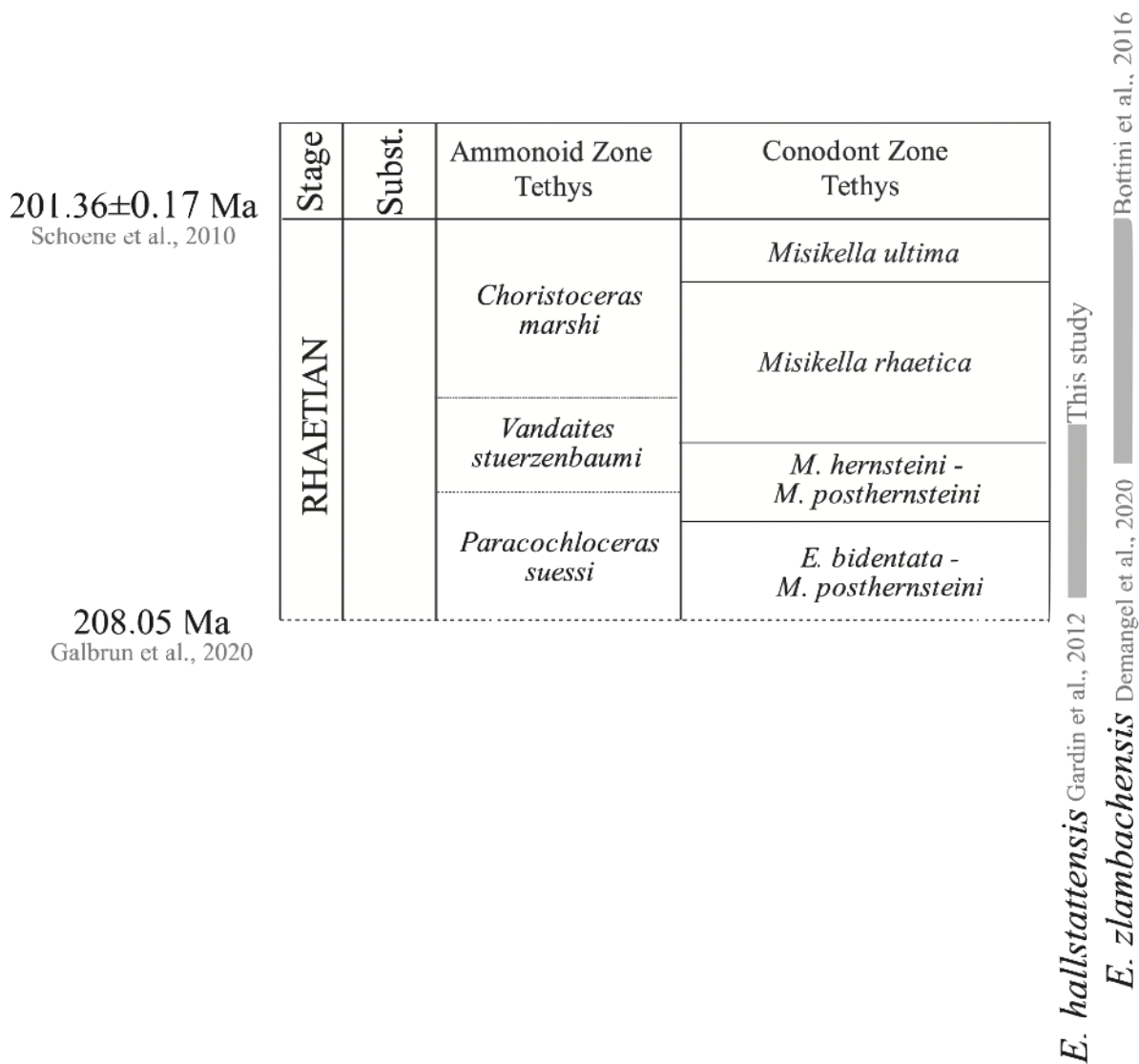


**Figure 3:** Rhaetian biozonation based on Tethyan ammonoids and conodonts (Galbrun et al., 2020; Ogg et al., 2020) along with the ranges of the *Eoconusphaera* species discussed here

**Differentiation:** *Eoconusphaera hallstattensis* and *E. zlambachensis* exhibit many similarities in SEM view, but have distinctly different organisation of the elements in the core, with irregularly overlapping vertical laths in *E. hallstattensis* and clearly oblique bundles of regularly arranged laths in *E. zlambachensis*. Also, *E. hallstattensis* does not show an axial suture under crossed nicols, while *E. zlambachensis* does. The two species can be easily distinguished in the LM due to their different inner structures. Finally, the two species are dominant in distinct stratigraphic intervals—*E. hallstattensis* is abundant in the Lower Rhaetian (*Paracochloceras suessi* to the base of the *Vandaites stuerzenbaumi* ammonoid zones; *Epigondolella bidentata*–*Misikella posthernsteini* and *M. posthernsteini*–*Misikella hernsteini* conodonts zones), while *E. zlambachensis* dominates in the Middle and Upper Rhaetian (*V. stuerzenbaumi* and *Choristoceras marshi* ammonoid zones; *Misikella rhaetica* and *M. ultima* conodont zones) (Figure 3).

*Eoconusphaera hallstattensis* differs from *C. jansae* (Wiegand, 1984), which occurs in the Sinemurian–Toarcian, by its disjunct stratigraphic level and distinctly different ultrastructure in the central core. *Calcivascularis jansae* has vertical laths in the lower part of the core, with a complex spine above this, which fills the central area, while *E. hallstattensis* has irregularly overlapping vertical laths filling the core.

**Remarks:** *Eoconusphaera hallstattensis* presents a broad range of size, from short and stubby (Pl. 1, figs 4, 17, 18) to tall and narrow (Pl. 1, figs 5, 16), with several medium-sized specimens in between (Pl. 1, figs 1, 6, 7, 9, 11–15). The thickness of the mantle and the inner laths can vary with preservation, with the appearance of the inner laths in the LM varying from long bars to small blocks. *Eoconusphaera hallstattensis* has a protolith outer wall, with small, low-rimmed specimens being only slightly taller than the similar protolith rim of *C. minutus*, suggesting they could be closely related.

**Holotype:** Pl. 1, fig. 1 (catalogue number 219913, collection of the Universalmuseum Joanneum, Department of Geology and Palaeontology, Graz, Austria).

**Dimensions:** Holotype length = 2.6  $\mu\text{m}$ ; holotype widest diameter = 1.6  $\mu\text{m}$ ; holotype narrowest diameter = 1.4  $\mu\text{m}$ . The height ranges from 2.0 or 2.4 (Pl. 1, fig. 17) to 5.8  $\mu\text{m}$ , while the width at the widest end varies from 1.1 to 3.1  $\mu\text{m}$  and at the narrowest end between 1.0 and 2.4  $\mu\text{m}$ .

**Paratypes:** Pl. 1, figs 2–5 (catalogue numbers 219913 [Sample Zl 6.4202 for paratype figs 2, 3, 5] and 219915 [Sample Zl 35.9311 for paratype fig. 4], collection of the Universalmuseum Joanneum, Department of Geology and Palaeontology, Graz, Austria).

**Type locality:** Kleiner Zlambach, NCA, Austria (section base: 46.6464°N, 13.673°E; section top: 46.6457°N, 13.6675°E).

**Type level:** Sample Zl 6.4202, 6.4 m above the base of the Kleiner Zlambach section, Lower Rhaetian (*P. suessi* ammonoid zone; *E. bidentata*–*M. posthernsteini* conodont zone), Upper Triassic.

**Geographical occurrence:** The oldest specimens reported so far are from the base of the Rhaetian in the Steinbergkogel section (Gardin et al., 2012). This species is rare in the Hallstatt Formation of the Steinbergkogel section (Demangel et al., 2020), but is common in the examined samples of the Zlambach Formation from the Kleiner Zlambach section



(both are located in the open-oceanic Hallstatt Basin, NCA, Austria). This species has also been recorded in the Kössen Formation (intraplatform Eiberg Basin, NCA, southern Germany: Janofske, 1987) and from ODP Leg 122 (Wombat Plateau, north-western Australia), where the species is present in low abundances (rare to few: Bralower et al., 1991; SG, unpublished data, 2017). It is common in the Lower Rhaetian in the NCB of Western Australia (RH, unpublished data, 2018).

**Stratigraphical occurrence:** This species ranges through the Rhaetian (Upper Triassic), from the *P. suessi* to *V. stuerzenbaumi* ammonoid zones (*E. bidentata*–*M. posthernsteini* to *M. rhaetica* conodont zones) in Austria and in the Lower Rhaetian (i.e. in the *Rhaetogonyaulax rhaetica* dinoflagellate zone) in Australia. The topmost occurrence of the species observed so far is in the upper *V. stuerzenbaumi* ammonoid zone/*M. rhaetica* conodont zone in the Zlambach Formation of the NCA, Austria.

*Eoconusphaera zlambachensis* (Moshkovitz, 1982) Bown & Cooper, 1989 emend.  
Demangel, Howe, Gardin & Richoz, Pl. 2, figs 1–17

1982 *Conusphaera zlambachensis* Moshkovitz: pp. 612– 613, pl. 1, figs 1–10 (holotype = figs 1–3).

1983 *Eoconusphaera tollmanniae* Jafar: pp. 228–229, figs 1–3, 6.

1987 *Conusphaera zlambachensis* Moshkovitz, 1982 – Janofske: p. 49, pl. 2, figs 6–8.

1987 *Conusphaera tollmanniae* (Jafar, 1982) Janofske: p. 49, pl. 2, figs 1–5.

1987 *Conusphaera zlambachensis* Moshkovitz, 1982 – Bown: p. 72, pl. 11, figs 1–3; pl. 15, figs 13, 14.

1987 *Conusphaera zlambachensis* Moshkovitz, 1982 – Posch & Stradner: p. 232, text-fig. 6, pl. 1, figs 1–7.

1988 *Eoconusphaera zlambachensis* (Moshkovitz, 1982) Kristan-Tollmann: p. 77,

1989 *Eoconusphaera zlambachensis* (Moshkovitz, 1982) Kristan-Tollmann, 1988 – Bown & Cooper: p. 104, pl. 5.1, figs 1–8.

1995 *Eoconusphaera zlambachensis* (Moshkovitz, 1982) - Kristan-Tollmann, 1988 – Kristan-Tollmann: pp. 2–4, pl. 1, figs 1–6.

2010 *Eoconusphaera zlambachensis* (Moshkovitz, 1982) Kristan-Tollmann, 1988 – Clémence et al.: fig. 11c, k.

2016 *Eoconusphaera zlambachensis* (Moshkovitz, 1982) Kristan-Tollmann, 1988 – Bottini et al.: figs 5–8.

**Derivation of name:** After the Zlambach Marl (now renamed the Zlambach Formation), where the first specimens were found.

**Original diagnosis:** “Elongated cone, truncated at both ends, composed of some 35–40 calcitic lamellae, closely packed and radiating from the center of the cone. When viewed from the narrower base, the lamellae are seen to be inclined and arranged in a sinistrally turning spindle (Pl. 1, Fig. 3, 4, 6 [in Moshkovitz, 1982; herein, Pl. 2, figs 2, 3, 5, 8]). The outer surface of the cone is covered by elongated, smooth plates, each one separated from

the other [herein, Pl.2, figs 2, 5, 7]. In LM, the form is too small to reveal the fine details of the lamellae and only the general conical shape and the cover plates, which in many specimens [sic.] have fallen out (Pl. 1, Fig. 4, 5 [in Moshkovitz, 1982]) could be discerned (Pl. 1, Fig. 7, 8 [in Moshkovitz, 1982]).”

**Emended description:** In addition to the presence of a core comprising approximately eight radially arranged bundles (Posch & Stradner, 1987), our observations highlighted additional characteristics, including the inclination of the calcite laths (between 150 and 159°; Pl. 2, figs 2, 5, 8). Similarly to *Eoconusphaera hallstattensis*, specimens have been observed with a domed shape at the widest extremity, formed by an extension of the inner laths (Pl. 2, figs 3, 5, 11, 14, 16), which can be enclosed by the outer mantle of elements, if these are preserved (Pl. 2, figs 3, 11, 12, 14). Less frequently, and only observed in the SEM, *E. zlambachensis* can also present a domed structure on the narrow extremity, formed by the outer mantle laths joining at the end, more or less enclosing the extremity, depending on preservation (Pl. 2, fig. 2). Under the LM, *E. zlambachensis* has a more trapezoid shape than *E. hallstattensis*. Because the laths of the inner core in *E. zlambachensis* are very thin (<0.5 µm thick), they cannot be distinguished from each other optically. Hence, the inner core appears as a homogenous, birefringent block at all angles to the polariser. A thin, dark line, reflecting the central axis, from which the laths of the inner core radiate, is visible in some orientations.

**Differentiation:** *Eoconusphaera zlambachensis* differs from *E. hallstattensis* in the inclination of the laths in the inner core, its appearance in the LM (see description above), its more circular extremities and its dominance in the *V. stuerzenbaumi* and *Choristoceras marshi* ammonoid zones (*M. rhaetica* and *M. ultima* conodont zones).

**Dimensions of observed specimens:** The length of our specimens varied between 2.2 and 4.8 µm, with the width of the wide end varying between 1.4 and 3 µm, and the width of the narrow end varying from 1 to 2.5 µm.

**Holotype dimensions:** Length = 8 µm; width of wide end = 5 µm; width of narrow end = 3.5 µm (Moshkovitz, 1982).

**Geographical occurrence:** According to Moshkovitz (1982), *E. zlambachensis* was common in the Zlambach Formation (open-oceanic Hallstatt Basin) in the Fischerwiese and Roßmoosgraben sections and less frequent in the Kössen Formation (intraplatform Eiberg Basin) in the Kendlbachgraben section. According to Jafar (1983), it was only frequent (not common) in the Fischerwiese section (Zlambach Formation) and rare in the Ampelsbach section (Kössen Formation). Bown & Cooper (1989) reported a high abundance (i.e. 10–20 specimens per field of view at 1000x magnification, equivalent to 50% of the assemblage) in the Weißloferbach section (Kössen Formation). According to Kristan-Tollmann (1995), the species was as common as *Prinsiosphaera triassica* in the Grünbachgraben section (Zlambach Formation). Clémence et al. (2010) reported its high relative abundance in the Eiberg section (i.e. 20–40% of the assemblages), but less abundant in Tiefengraben (i.e. 10–15%, both in the Kössen Formation). All these localities are in the NCA, Austria. Bralower et al. (1991) recorded this species as being common in the Upper Triassic of the Wombat Plateau, offshore Western Australia. It was very common (up to 100–150 specimens per field of view at 1000x magnification) in the

Brigadier Formation in the NCB, offshore Western Australia (RH, unpublished data, 2018).

**Stratigraphical occurrence:** Upper Triassic, Rhaetian (lower *V. stuerzenbaumi*–*C. marshi* ammonoid zones, *M. posthernsteini*–*M. hernsteini* to *M. ultima* conodont zones).

**Remarks:** The specimens called *E. z lambachensis* by Bralower et al. (1991) do not closely resemble the holotype of this species. The inner core of their specimens, figured in LM photomicrographs (Bralower et al., 1991, pl. IX, figs 7–11), do not have the typical continuous birefringence pattern of *E. z lambachensis*, so they are considered here to belong to *E. hallstattensis*. The specimens illustrated by Bottini et al. (2016, pl. 1, figs 5–8) are poorly preserved, but in the LM, they show continuous laths in the core, suggesting they are closer to *E. z lambachensis* than *E. hallstattensis*, which has discontinuous laths in the core.

#### 4. Conclusions

This study clarifies the taxonomy of the two species in the genus *Eoconusphaera* in the Late Triassic. A new species—*Eoconusphaera hallstattensis*—has been described as having two differentiating characteristics—the absence of an axial suture under crossed nicols and the presence of numerous overlapping, vertical inner laths, which appear as undulating bars in the LM. *Eoconusphaera z lambachensis* has been emended to include specimens where the inner, inclined (~154°) laths are arranged in bundles; it also sometimes has a domed shape at the wider end, like *E. hallstattensis*, but also, less frequently, at the narrow end. In addition to the different structural characteristics (inner lath shape and orientation), these two species dominate in different stratigraphic intervals. *Eoconusphaera hallstattensis* first occurs in the *Paracochloceras suessi* ammonoid zone, dominating from there up to the base of the *Vandaites stuerzenbaumi* ammonoid zone. *Eoconusphaera z lambachensis* first appears at the base of the *V. stuerzenbaumi* zone and dominates during that and the *Choristoceras marshi* zone. We suggest that these two species might be useful biostratigraphic markers for the latest Triassic in the Western Tethys.

#### Acknowledgements

This research was supported by the Austrian Science Foundation (Project P 29497-P29 to SR). The SEM observations were supported by the Royal Physiographic Society of Lund (grant to ID). We thank Werner E. Piller for his advice on the taxonomic description and his help in improving the English in the early stages of the manuscript. We very much thank Dr Jeremy Young for his careful review, his suggestions, and his help in integrating the crystallographic orientation analyses to improve the manuscript. We also thank Matt Hampton for his critical comments and interesting interpretations.

#### References

- Bordiga, M., Bartol, M. & Henderiks, J. 2015. Absolute nannofossil abundance estimates: Quantifying the pros and cons of different techniques. *Revue de Micropaléontologie*, **58**: 155–165. 10.1016/j.revmic.2015.05.002
- Bottini, C., Jadoul, F., Rigo, M., Zaffani, M., Artoni, C. & Erba, E. 2016. Calcareous nannofossils at the Triassic/Jurassic boundary: Stratigraphic and paleoceanographic characterization. *Rivista Italiana di Paleontologia e Stratigrafia*, **122**(3): 141–164. 10.13130/2039-4942/7726

- Bown, P.R. 1987. Taxonomy, evolution, and biostratigraphy of Late Triassic–Early Jurassic calcareous nannofossils. *Special Papers in Paleontology*, **38**: 1–118.
- Bown, P.R. & Cooper, M.K.E. 1989. Conical calcareous nannofossils in the Mesozoic. In: J.A. Crux & S.E. Heck (Eds). *Nannofossils and their applications*. British Micropalaeontology Society, Ellis Horwood, Chichester: 98–106.
- Bown, P.R. & Young, J.R. 1998. Techniques. In: P.R. Bown (Ed.). *Calcareous nannofossil biostratigraphy*. British Micropalaeontological Society Publications Series/Chapman & Hall/Kluwer Academic, London: 16–21.
- Bralower, T.J., Bown, P.R. & Siesser, W.G. 1991. Significance of Upper Triassic nannofossils from the Southern Hemisphere (ODP Leg 122, Wombat Plateau, N.W. Australia). *Marine Micropaleontology*, **17**: 119–154. 10.1016/0377-8398(91)90025-2
- Clémence, M.E., Gardin, S., Bartolini, A., Paris, G., Beaumont, V. & Guex, J. 2010. Benthoplanktonic evidence from the Austrian Alps for a decline in sea-surface carbonate production at the end of the Triassic. *Swiss Journal of Geosciences*, **103**: 293–315. 10.1016/j.palaeo.2010.05.021
- Demangel, I., Kovacs, Z., Richoz, S., Gardin, S., Krystyn, L., Baldermann, A. & Piller, W.E. 2020. Development of early calcareous nanoplankton in the Northern Calcareous Alps (Austria) in the Late Triassic. *Global and Planetary Change*, **193**: 103254. 10.1016/j.gloplacha.2020.103254
- Galbrun, B., Boulila, S., Krystyn, L., Richoz, S., Gardin, S. & Bartolini, A. 2020. “Short” or “long” Rhaetian? Astronomical calibration of Austrian key sections. *Global and Planetary Change*, **192**: 103253. 10.1016/j.gloplacha.2020.103253
- Gallet, Y., Besse, J., Krystyn, L. & Marcoux, J. 1996. Norian magnetostratigraphy from the Scheiblkogel section, Austria: Constraint on the origin of the Antalya Nappes, Turkey. *Earth and Planetary Science Letters*, **140**(1–4): 113–122. 10.1016/0012-821X(96)00044-1
- Gardin, S., Krystyn, L., Richoz, S., Bartolini, A. & Galbrun, B. 2012. Where and when the earliest coccolithophores? *Lethaia*, **45**: 507–523. 10.1111/j.1502-3931.2012.00311.x
- Golonka, J. 2007. Late Triassic–Early Jurassic palaeogeography of the world. *Palaeogeography, Palaeoclimatology, Palaeoecology*, **244**: 297–307. 10.1016/j.palaeo.2006.06.041
- Helby, R., Morgan, R. & Partridge, A.D. 1987. A palynological zonation of the Australian Mesozoic. In: P.A. Jell (Ed.). *Studies in Australian Mesozoic Palynology*. Association of Australasian Palaeontologists Memoir, **4**: 1–85.
- Helby, R., Morgan, R. & Partridge, A.D. 2004. *Updated Jurassic–Early Cretaceous dinocyst zonation NWS Australia*. Geoscience Australia publication ISBN 1 920871 01 2.
- Jafar, S.A. 1983. Significance of Late Triassic calcareous nanoplankton from Austria and southern Germany. *Neues Jahrbuch für Geologie und Paläontologie*, **166**: 218–259.
- Janofske, D. 1987. Kalkige Nannofossilien aus der Ober-Trias (Rhät) der Nördlichen Kalkalpen. *Berliner Geowissenschaftliche Abhandlungen*, **86**: 45–67.
- Kovacs, Z., Demangel, I., Richoz, S., Hippler, D., Baldermann, A. & Krystyn, L. 2020. New constraints on the evolution of  $^{87}\text{Sr}/^{86}\text{Sr}$  of seawater during the Upper Triassic. *Global and Planetary Change*, **192**: 103255. 10.1016/j.gloplacha.2020.103255

- Kristan-Tollmann, E. 1988. Coccolithen aus den älteren Allgäuschichten (alpiner Lias, Sinemur) von Timor, Indonesian. *Geologisch-Paläontologische Mitteilungen Innsbruck*, **15**: 71–83.
- Kristan-Tollmann, E. 1995. Weitere Beobachtungen an Rhätischen Nannofossilien der Tethys. *Geologisch-Paläontologische Mitteilungen Innsbruck*, **20**: 1–11.
- Marshall, N. & Lang, S. 2013. A new sequence stratigraphic framework for the North West Shelf, Australia. In: M. Keep & S.J. Moss (Eds). *The Sedimentary Basins of Western Australia 4: Proceedings of the Petroleum Exploration Society of Australia Symposium*. Petroleum Exploration Society of Australia, Perth: 1–32.
- Moshkovitz, S. 1982. On the findings of a new calcareous nannofossil (*Conusphaera zlabachensis*) and other calcareous organisms in the Upper Triassic sediments of Austria. *Eclogae Geologicae Helvetiae*, **75**: 611–619. 10.5169/seals-165245
- Nakada, R., Ogawa, K., Suzuki, N., Takahashi, S. & Takahashi, Y. 2014. Late Triassic compositional changes of eolian dusts in the pelagic Panthalassa: Response to the continental climatic change. *Palaeogeography, Palaeoclimatology, Palaeoecology*, **393**: 61–75. 10.1016/j.palaeo.2013.10.014
- Ogg, J.G., Chen, Z.-Q., Orchard, M.J. & Jiang, H.S. 2020. The Triassic Period. In: F.M. Gradstein, J.G. Ogg, M.D. Schmitz & G.M. Ogg (Eds). *The Geologic Time Scale 2020*. Amsterdam, Elsevier: 903–953. 10.1016/B978-0-12-824360-2.00025-5
- Posch, F. & Stradner, H. 1987. Report on Triassic Nannoliths from Austria. *Abhandlungen der Geologischen Bundesanstalt*, **39**: 231–237.
- Preto, N., Agnini, C., Rigo, M., Sprovieri, M. & Westphal, H. 2013a. The calcareous nannofossil *Prinsiosphaera* achieved rock-forming abundances in the latest Triassic of western Tethys: Consequences for the  $\delta^{13}\text{C}$  of bulk carbonate. *Biogeosciences*, **10**: 6053–6068. 10.5194/bg-10-6053-2013
- Preto, N., Willems, H., Guaiumi, C. & Westphal, H. 2013b. On- set of significant pelagic carbonate accumulation after the Carnian Pluvial Event (CPE) in the western Tethys. *Facies*, **59**: 891–914. 10.1007/s10347-012-0338-9
- Richoz, S. & Krystyn, L. 2015. The Upper Triassic events recorded in platform and basin of the Austrian Alps. The Triassic/Jurassic GSSP and Norian/Rhaetian GSSP candidate. *Berichte der Geologischen Bundesanstalt*, **111**: 75–137.
- Schoene, B., Guex, J., Bartolini, A., Schaltegger, U. & Blackburn, T.J. 2010. Correlating the end-Triassic mass extinction and flood basalt volcanism at the 100 ka level. *Geology*, **35**(5): 387–390. 10.1130/G30683.1
- Scotese, C.R. 2004. A continental drift flipbook. *Journal of Geology*, **112**: 729–741. 10.1086/424867
- Turland, N.J., Wierema, J.H., Barrie, F.R., Greuter, W., Hawksworth, D.L., Herendeen, P.S., Knapp, S., Kusber, W.-H., Li, D.-Z., Marhold, K., May, T.W., McNeill, J., Monro, A.M., Prado, J., Price, M.J. & Smith, G.F. (Eds) 2018. *International Code of Nomenclature for algae, fungi, and plants (Shenzhen Code) adopted by the Nineteenth International Botanical Congress, Shenzhen, China, July 2017*. Regnum Vegetabile 159. Glashütten, Koeltz Botanical Books. 10.12705/Code.2018

Wiegand, G.E. 1984. Two new genera of calcareous nannofossils from the Lower Jurassic. *Journal of Paleontology*, **58**(4): 1151–1155.

Woodside Energy Ltd. 2007a. *Well completion report, Pluto-3 & ST1 basic data (WA-350-P, Carnarvon Basin)*. Woodside Energy Ltd., unpublished report. Available from [www.nopims.ga.gov.au](http://www.nopims.ga.gov.au)

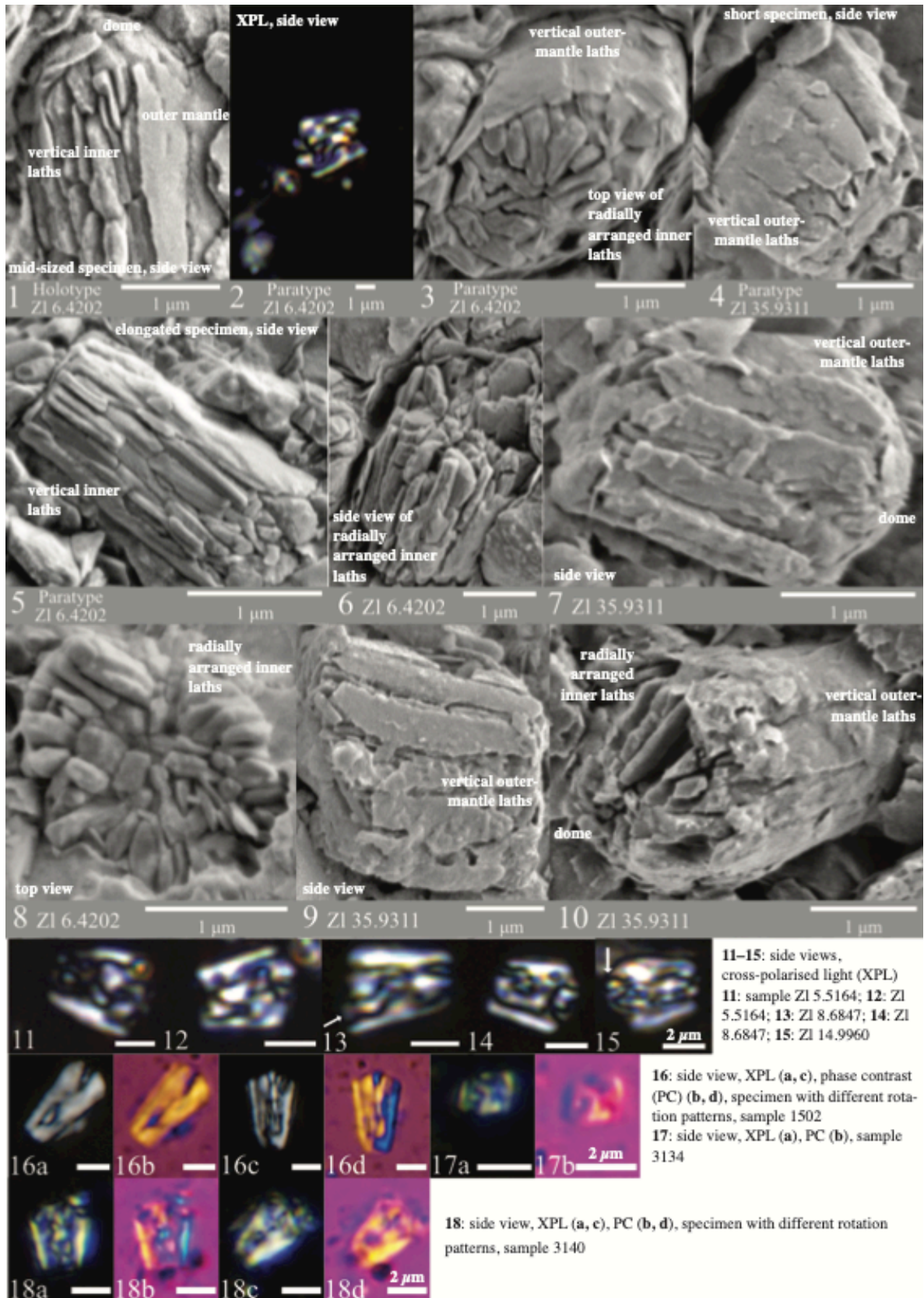
Woodside Energy Ltd. 2007b. *Well completion report, Pluto-4 basic data (WA-350-P, Carnarvon Basin)*. Woodside Energy Ltd., unpublished report. Available from [www.nopims.ga.gov.au](http://www.nopims.ga.gov.au)

Young, J.R., Didymus, J.M., Bown, P.R., Prins, B. & Mann, S. 1992. Crystal assembly and phylogenetic evolution in heterococcoliths. *Nature*, **356**: 516–518.

Young, J.R., Teale, C.T. & Bown, P.R. 1986. Revision of the stratigraphy of the Longobucco Group (Liassic, southern Italy); based on new data from nannofossils and ammonites. *Eclogae Geologicae Helvetiae*, **79**(1): 117–135.

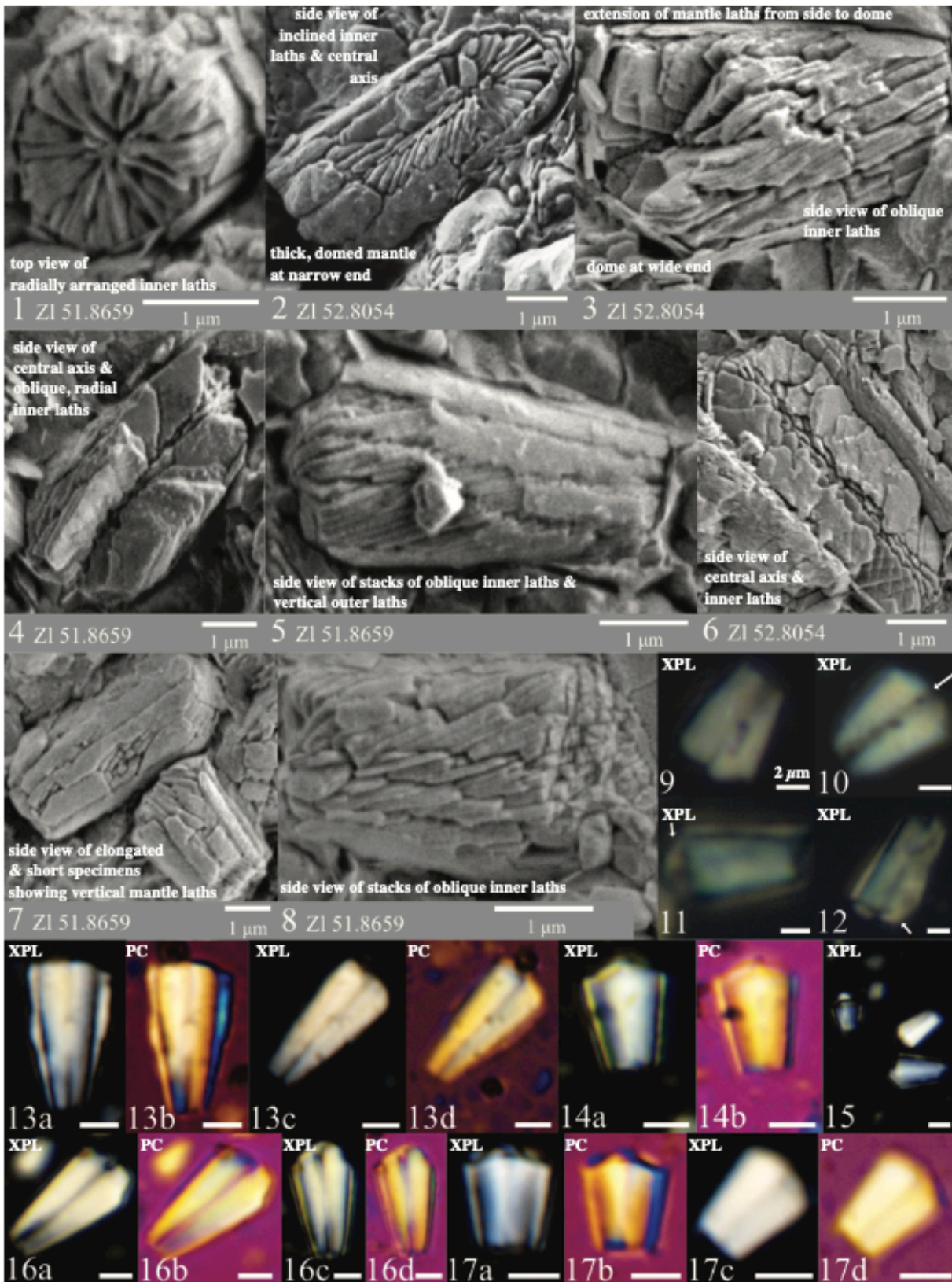
# Plate 1

*Eoconusphaera hallstattensis* SEM & LM images. 1–15: Zlambach, Austria; 16–18: Australia



## Plate 2

*Eoconusphaera zlambachensis* SEM & LM images. 1–12: Zlambach, Austria;  
13–17: Australia



9–12: side views of four specimens with a dome shape at the wide end, mantle visible as pale lateral bars, central axis dark, sample ZI 51. 8659. 13: side view of specimen with different rotation patterns, sample 1499. 14: side view, sample 3143. 15: side view of three specimens, sample 3150. 16: side view of specimen with different rotation patterns, sample 3146. 17: side view of specimen with different rotation patterns, sample 1501